



Use of [¹⁸F]FDG PET/CT for Target Volume Definition in Radiotherapy

1

Johanna E. E. Pouw, Dennis Vriens, Floris H. P. van Velden,
and Lioe-Fee de Geus-Oei

Abbreviations

ATLAAS	Automatic decision Tree-based Learning Algorithm for Advanced Segmentation
ATP	Adenosine-5'-TriPhosphate

The original version of the chapter was revised. A correction to this chapter can be found at https://doi.org/10.1007/978-3-031-08601-4_14

J. E. E. Pouw (✉)

Section of Nuclear Medicine, Department of Radiology, Leiden University Medical Center (LUMC), Leiden, The Netherlands

HollandPTC, Delft, The Netherlands

Department of Medical Oncology, Amsterdam UMC location Vrije Universiteit Amsterdam, Amsterdam, The Netherlands

e-mail: J.E.E.Pouw@amsterdamumc.nl

D. Vriens

Section of Nuclear Medicine, Department of Radiology, Leiden University Medical Center (LUMC), Leiden, The Netherlands

HollandPTC, Delft, The Netherlands

e-mail: D.Vriens@lumc.nl

F. H. P. van Velden

Section of Nuclear Medicine, Department of Radiology, Leiden University Medical Center (LUMC), Leiden, The Netherlands

e-mail: F.H.P.van_Velden@lumc.nl

L.-F. de Geus-Oei

Section of Nuclear Medicine, Department of Radiology, Leiden University Medical Center (LUMC), Leiden, The Netherlands

Biomedical Photonic Imaging Group, University of Twente, Enschede, The Netherlands

e-mail: L.F.de_Geus-Oei@lumc.nl

CT	X-ray Computed Tomography
CTAC	(low dose) CT performed for Attenuation- and scatter Correction of the PET-image
CT-TV	CT-only based Target Volume
CTV	Clinical Target Volume
EANM	European Association of Nuclear Medicine
EARL	EANM Research Ltd.
EORTC	European Organisation for Research and Treatment of Cancer
ESTRO	European Society for Radiotherapy and Oncology
FBP	Filtered Backprojection Reconstruction Algorithm
[¹⁸ F]FDG	2-[¹⁸ F]fluoro-2-deoxy-D-Glucose
GTV	Gross Tumour Volume
HNSCC	Head-and-Neck Squamous Cell Carcinoma
LOR	Line-Of-Response
MRI	Magnetic Resonance Imaging
NSCLC	Non-Small Cell Lung Carcinoma
OAR	Organs At Risk
OSEM	Ordered Subsets Expectation Maximisation reconstruction algorithm
PET	Positron Emission Tomography
PET-AS	Automatic Segmentation of contours in PET
PET-TV	PET/(CT)-based Target Volume
Planning-CT	(High dose, contrast-enhanced) CT performed for radio therapy treatment planning purpose
PTV	Planning Target Volume
STAPLE	Simultaneous Truth and Performance Level Estimate
SUV	Standardised Uptake Value
SCLC	Small Cell Lung Carcinoma

1.1 Introduction

High-precision radiotherapy is of increasing importance in oncological treatment, by striving for higher effectiveness and decreasing side effects by more conformal dose delivery. This can be accomplished by new X-ray photon radiotherapy techniques, including volumetric-modulated arc therapy (Chap. 5) and intrafraction adaptation using the magnetic resonance-based linear accelerator (Chaps. 6 and 7), by particle therapy (protons, carbon ions; Chap. 10), or by highly precise target volume definition, which will be the focus of the current chapter.

Different phases can be distinguished in the development of a treatment plan. First, accurate information about the localisation and extension of the tumour volume, with respect to its surroundings, should be obtained, the so-called gross tumour volume (GTV). This information is obtained by a combination of different diagnostic methods, including physical examination (visual inspection, palpation), medical imaging [endoscopy, (endo)ultrasonography, computed tomography (CT), magnetic resonance imaging (MRI), and positron emission tomography (PET)], and cytology or histopathology. Second, the information of these different modalities

needs to be properly co-registered to the CT scan used for treatment planning purposes. Third, the target volumes are defined on the planning CT: GTV is defined as the tumour visible (or palpable) on physical examination or imaging. The clinical target volume (CTV) takes into account the microscopic tumour extension and the planning target volume (PTV) includes additionally systematic and random setup inaccuracies, resulting in the volume to be irradiated. These margins make the planning more reliable, but also account for a smaller therapeutic window [1]. The definitions of the target volumes are defined in International Commission on Radiation Units and Measurements (ICRU) Report 50 [2]. Also, the organs at risk (OAR), in which the radiation dose is to be maximally reduced, are segmented on the images. Finally, a treatment plan is generated, taking into account geometric (e.g. motion, patient setup-variability) and physical (e.g. particle range) uncertainties.

Image contrast in the planning-CT, which is ideally acquired in radiotherapy position, is determined by differences in photon attenuation of various tissues and thereby delivers anatomical (geometrical) information. The (semi)quantitative information on photon attenuation can be used to estimate the behaviour of high-energy photons in human tissues and thus to reliably calculate radiation treatment plans. CT, however, suffers from limited soft-tissue contrast, which can for a limited extent be overcome by the addition of intravenous iodinated contrast media. Additional imaging by other imaging modalities can assist in more accurate segmentation of the target volume. MRI is based on a different physical property of tissues: its nuclear magnetic spin resonance. Conventional MRI-sequences result in anatomical images of higher soft tissue contrast, compared to CT, but might, just as CT, be flawed by artefacts including magnetic susceptibility (metal implants), geometrical distortions, motion and flow (perfusion).

PET provides biological information of the tumours and organs at risk, which can be co-registered to the anatomical domain of CT or MRI. Current standard-of-care is the combination of PET with CT. Although PET/MRI is currently available, clinical application in radiotherapy planning is not yet widely implemented due to technical challenges, such as accurate MRI-based attenuation correction of the PET-images (see later) and geometrical distortions of the MRI [3–5]. Which biological information is obtained by PET-imaging depends on the administered radiopharmaceutical (“tracer”). This chapter will cover the use of the most widely used PET-radiopharmaceutical 2-[¹⁸F]fluoro-2-deoxy-D-glucose ([¹⁸F]FDG). The usage of this specific radiopharmaceutical can be assumed when PET is mentioned in the remainder of this chapter. Chapter 2 will cover the use of PET tracers beyond [¹⁸F]FDG.

To gain insight into the additional value of PET in target volume delineation (TVD), first, the basic principles of PET/CT and the radiopharmaceutical [¹⁸F]FDG will be discussed, followed by the image acquisition and reconstruction techniques, including methods for motion control (“Technical Aspects”). The role of [¹⁸F]FDG PET/CT in tumour volume and lymph node segmentation, together with its value in different disease sites will be discussed in “Target volume delineation”. The influence of the applied segmentation method is discussed in “PET/CT segmentation methods” and the risks and disadvantages of the application of PET will be highlighted in section “Cons and pitfalls”. The chapter will end with a future perspective on the role of [¹⁸F]FDG PET/CT in treatment planning.

Out of the scope of this chapter is the established role of [¹⁸F]FDG PET/CT in determining the extent of different oncological diseases (staging), the use of

[¹⁸F]FDG PET/CT as prognostic biomarker and predictor of treatment response and its role in detection of tumour recurrence after treatment (follow-up).

1.2 [¹⁸F]FDG PET/CT

1.2.1 PET/CT

The unstable nucleus of the isotope bound to the radiopharmaceutical, fluorine-18 in the case of [¹⁸F]FDG, emits a positron (β^+) when it decays. This positron will slow down in the tissue around its origin and will interact with any of the electrons (e^-) in the tissue within a few millimetres from its origin. As positrons are the anti-particles of electrons, collision of positrons and electrons will result in disappearance of both particles, so-called annihilation, releasing energy in the form of two (nearly) anti-parallel 511 keV photons. By detecting these coincident, paired photons with a PET-camera, a line can be derived on where the annihilation took place, a so-called line-of-response (LOR). When enough LORs are measured, the origin of the annihilation can be retraced using a reconstruction algorithm, resulting in the spatial distribution of the radiopharmaceutical, i.e. a PET-image (Fig. 1.1). Most current PET/CT scanners have time-of-flight capabilities that can register the arrival time of each of both photons on a detector separately, allowing further localisation (with a certain probability) of the point of annihilation on the LOR. Current clinical scanners have time-of-flight coincidence timing resolutions below 210 ps, translating to a position uncertainty of less than 31.5 mm [6].

The magnitude of the signal depends on the number of degradations observed by the camera. This in turn is dependent on the concentration of the radiopharmaceutical, thus the pharmacokinetics of the injected radiopharmaceutical and the probability that a photon-pair is detected by the PET camera. The latter is, apart from detector sensitivity and scanner geometry, mainly limited by photon absorption (attenuation) in the tissue that both annihilation photons have to traverse before reaching the detector ring, which can be measured by CT. Therefore, for the purpose of attenuation correction and anatomical localisation, a low-dose CT is performed, usually immediately prior to PET-acquisition.

In order to obtain images of acceptable image quality, sufficient LORs need to be measured and, therefore, whole-body PET-acquisition is a time-consuming process, typically in the order of 15-30 min, to keep the injected amount of radiopharmaceutical, and thus the effective radiation dose for the patient, within reasonable limits.

1.2.2 [¹⁸F]FDG

The most frequently used radiopharmaceutical for PET-imaging is [¹⁸F]FDG [7]. The isotope ¹⁸F mainly (96.9%) decays by β^+ -emission, with a decay half-life of 109.7 min and a maximum (mean) positron energy of 634 (250) keV. The resulting maximum (mean) positron range in water is 2.4 (0.6) mm before the annihilation, localised by PET/CT, takes place [8].

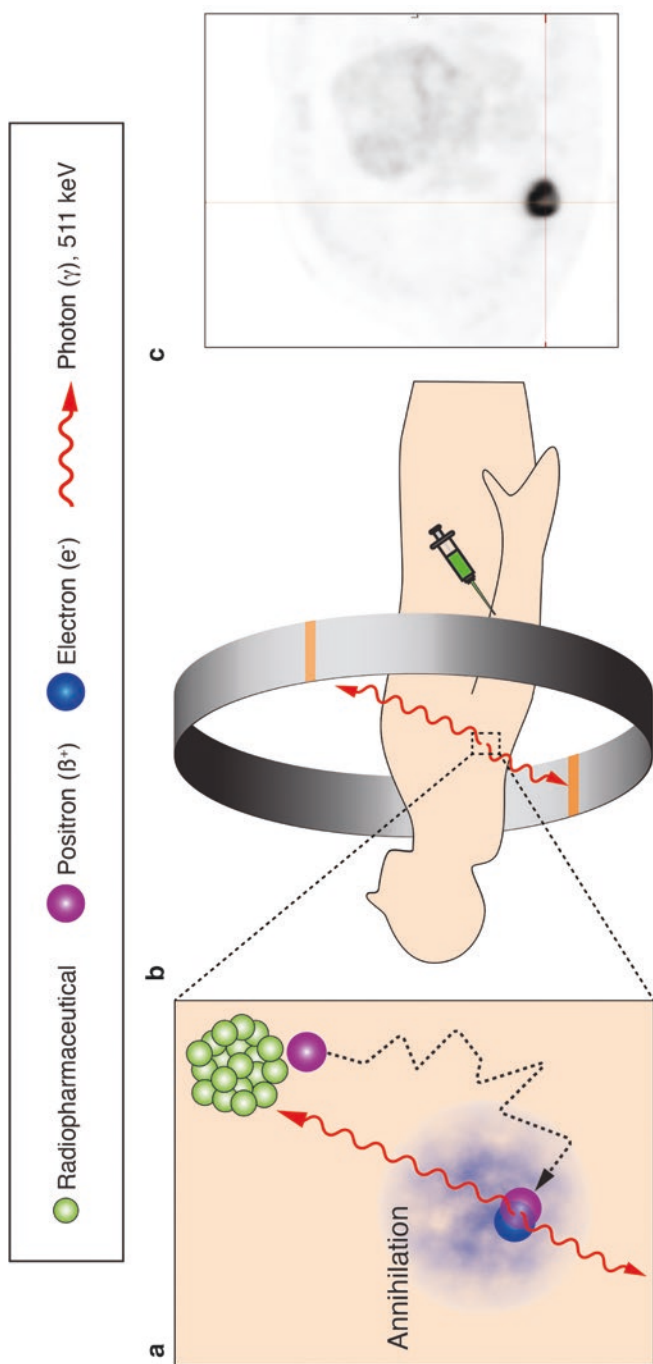


Fig. 1.1 The formation of a PET-image. (a) Electron–positron annihilation in the body within a few mm from the location of the radiopharmaceutical, resulting in two nearly antiparallel 511 keV photons. (b) Coincidence detection of the paired annihilation photons by the PET detector. (c) Example of an attenuation and scatter corrected PET-image, visualising a non-small cell lung carcinoma

[^{18}F]FDG is a radiopharmaceutical analogue to glucose. [^{18}F]FDG is transported by the blood stream, freely passes the vessel wall and extravascular extracellular space similar to D-glucose, the natural occurring form of glucose. There it is actively transported over the cellular membrane mainly by the sodium-dependent glucose transporter molecule family and is subsequently phosphorylated to [^{18}F]FDG-6-phosphate by the hexokinase enzyme family in the cytosol. For both [^{18}F]FDG and D-glucose the kinetics of these processes are nearly identical. Glucose-6-phosphate is catabolised to fructose-6-phosphate in the glycolysis pathway and eventually to two molecules of pyruvate. However, the enzyme responsible for this chemical reaction is not sensitive to [^{18}F]FDG-6-phosphate. As a result, [^{18}F]FDG-6-phosphate cannot be degraded further and, as dephosphorylation does not occur in most mammalian tissues, accumulates in the cells (Fig. 1.2). Therefore, [^{18}F]FDG uptake is

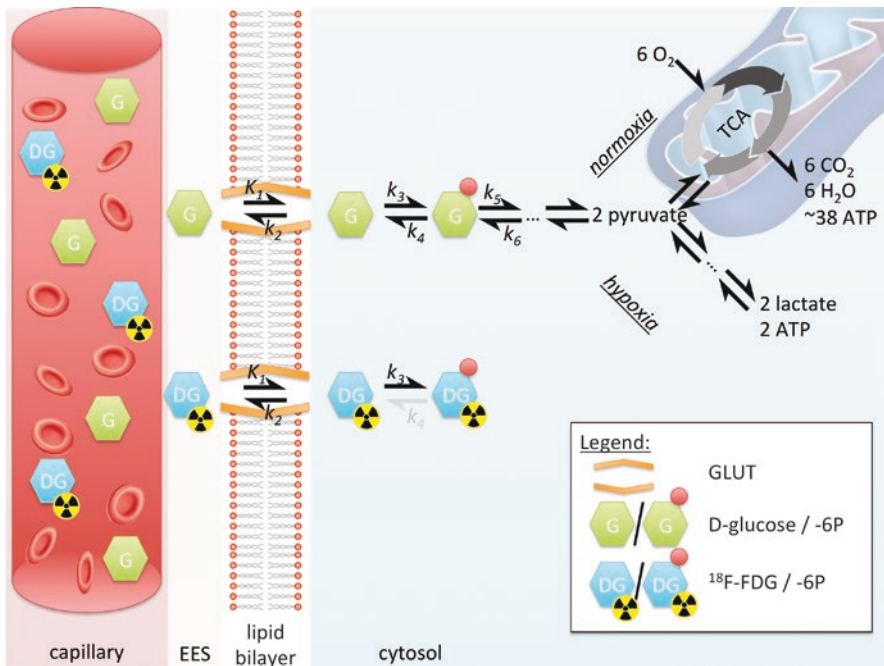


Fig. 1.2 The membrane-bound GLUT receptor family can reversibly transport both D-glucose and [^{18}F]FDG over the lipid bilayer of the cell. In the cytosol both D-glucose and [^{18}F]FDG are 6-phosphorylated by the hexokinase isozymes. In contrast to D-glucose-6-phosphate, [^{18}F]FDG-6-phosphate is not a substrate for the subsequent isomerase enzyme in the glycolytic pathway and, as 6-dephosphorylation hardly occurs in most mammalian tissues, its downstream products cannot enter the TCA-cycle. As a result, [^{18}F]FDG-6-phosphate will time-dependently accumulate in the cytosol, reflecting enzymatic activities and facilitating PET visualisation of high glucose demanding tissues. *ATP* adenosine-5'-triphosphate; *CO₂* carbon dioxide; *EES* extravascular extracellular space; [^{18}F]FDG 2-[^{18}F]fluoro-2-deoxy-D-glucose; *GLUT* facilitative membrane-bound sodium-independent glucose transporters; *H₂O* water; *K₁-k₆* equilibrium Michaelis-Menten rate constants; *O₂* oxygen; *TCA* tricarboxylic acid (or Krebs) cycle. Adapted from ISBN13/EAN 978-94-6108-927-4 (ch.1, p.xxii) © 2015 Dennis Vriens. All Rights Reserved

increased in tissues with high glucose metabolism, often the case in brain and myocardium, but also in cancerous lesions and inflammatory conditions.

Tumour cells acquire their adenosine-5'-triphosphate (ATP), the energy carrier necessary for mitosis, from the inefficient anaerobic glycolysis, i.e. from pyruvate to lactate instead of mitochondrial oxidative phosphorylation, i.e. from pyruvate to carbon dioxide, even when oxygen is plentiful. The former yields 18–19x less ATP than the latter. Due to this so-called Warburg effect, higher D-glucose metabolism is required for sufficient ATP availability. This glucose demand is further increased by the high cell proliferation [9].

1.3 Technical Aspects

To obtain high-quality images and to prevent large inter-investigation variability, standardised patient preparation and image acquisition and reconstruction are of uttermost importance. To ensure high-quality images and to overcome inter-investigational variability in PET imaging, procedure guidelines are defined by the European Association of Nuclear Medicine (EANM) [10] and monitored for multi-centre [¹⁸F]FDG PET/CT study purposes in the EANM Research Ltd. (EARL) accreditation programme [11].

1.3.1 Patient Preparation

To ensure proper visualisation of the regions of interest, [¹⁸F]FDG should specifically accumulate in the regions of interest. Uptake of [¹⁸F]FDG should be prevented in non-malignant tissues, such as active muscles and brown fat, by proper patient preparation. Patients should refrain from strenuous muscle activity before [¹⁸F]FDG-injection and from any muscle activity after [¹⁸F]FDG-injection. To prevent uptake in thermogenic brown-adipose tissue and muscle uptake by shivering, the resting period after injection of the radiopharmaceutical takes place in a warm environment. A stable normoglycaemic, hypoinsulinaemic situation should be strived for by injecting [¹⁸F]FDG only in patients who fasted for at least 4–6 h, are normoglycaemic (generally a serum glucose up to 11.1 mmol/L (i.e. 200 mg/dl) is accepted) and have not been injected with short-acting insulins for at least 4 h. Adequate hydration and voiding directly prior to PET/CT acquisition ensure fast clearance of the radiopharmaceutical and thus decrease dose to the patients, and prevent artefacts around the kidneys, ureters and urinary bladder. When the area to be imaged is located near the bladder, diuretic medication can be administered to further stimulate the emptying of the bladder during acquisition. To prevent metal artefacts, the patients are asked to remove all metal objects [10].

1.3.2 Image Acquisition and Reconstruction

After acquisition of the raw PET-data, reconstruction can be performed by mainly two methods, namely filtered backprojection (FBP) and iterative reconstruction. In FBP, the LORs are literally backprojected to recalculate the position of the [^{18}F]FDG-containing structure. Currently, the most commonly applied reconstruction technique in the clinical setting is iterative reconstruction. This method outperforms FBP by its high signal-to-noise ratio, the exclusion of counts outside the field of view and the multiple correction options within the reconstruction, e.g. time-of-flight correction.

These advantages most often outweigh the computational intensiveness of the reconstruction and the unpredictability of the nonlinear method. Iterative reconstruction is an iterative process of adjusting an estimated image, and is based on the difference between the estimated image of the projection data with the measured projection data. The most well-known example of iterative reconstruction is the ordered subsets expectation maximisation algorithm (OSEM), where the computational intensiveness is decreased by using only a subset of the projection angles in every iteration. This process is repeated over all subsets to ultimately perform one true iteration of OSEM [12]. A more extensive, but accessible, explanation of the reconstruction methods can be found in Cherry et al. [12].

Before reconstructing the raw PET-data, corrections need to be applied for several physical factors to obtain a true reflection of the radioactivity distribution of the radiopharmaceutical. The most important corrections are variations in coincidence detection efficiency between the different LORs (normalisation), dead time of the detector after a coincidence, random coincidence photons, scattered coincidence photons, and absorbed (attenuated) coincidence photons. As explained before, a low dose CT, acquired without contrast and often prior to PET-acquisition, is used for the attenuation correction of these coincidences and is also called the attenuation correction CT (CTAC). The amount of attenuation of 511 KeV annihilation photons depends on the (electron) density of the tissue. The photons will be more attenuated when passing through denser material, i.e. components with higher Hounsfield units, or when traversing more material, i.e. a larger body part [13].

1.3.3 Fusion and Registration of Treatment Planning PET/CT

1.3.3.1 Registration PET with CTAC

For correct anatomical localisation and attenuation- and scatter correction, the (low dose) CTAC and the PET need to be spatially aligned. Spatial mismatch between the PET and the CTAC results in incorrect attenuation correction and thereby scatter correction. This incorrect correction causes over- or underestimation of activity concentrations of the radiopharmaceutical (i.e. intensity), which is used to define the boundaries of the target volume on PET. Therefore, inaccurate attenuation- and scatter correction, due to spatial mismatch, also leads to inadequate information for target volume delineation.

Currently, all clinical PET/CT-scanners are dual-modality imaging devices, where the hardware accurately aligns the images of PET and CT, provided that no patient movement between the CTAC-acquisition and PET-acquisition has occurred. When (a large amount of) patient movement has occurred, PET and CT images have to be co-registered after acquisition, by translation, rotation and rescaling (rigid transformations) or by image deformation (non-rigid or elastic transformations), briefly summarised as “image registration” [14].

1.3.3.2 Registration PET/(CT) with Planning-CT

Biological information from the PET-image can be used for treatment planning by fusing either a staging PET or, preferably, a PET in treatment position with the high-dose and often contrast-enhanced planning-CT. In case of spatial mismatch between the PET and the planning-CT, improper functional-anatomical co-localisation may occur, resulting in inaccurate target volume definition. This can be overcome by manual co-registration focussing on the GTV and thus the volume planned to receive the high radiation dose. If misalignment persists, target volume coverage may be compromised, increasing the risk of geometrical miss. Therefore, the registration needs to be verified by an experienced radiation oncologist.

Imaging on different modalities increases the chance of inaccurate fusion by differences in time frames, patient position and coordinate systems [15]. Acquisition of both scans on the same machine and preferably at the same time would, therefore, minimise the spatial mismatch, but is often not realistic in clinical practice. When the planning-CT is obtained on the PET-system, this PET/CT-system needs to fulfil the quality assurance for treatment planning and thus needs to be regularly checked for its technical specifications, such as table rigidity and levelness, accurate laser alignment, and CT image matrix alignment [16]. Due to these additional, frequent quality controls on the one hand and device capacity on the other, multiple institutions use a stand-alone CT-scanner, instead of a hybrid PET/CT to perform a planning-CT.

The PET/CT for clinical diagnosis and staging purposes (*staging* PET/CT) is often one of the first steps in the clinical work-up before the decision for treatment modality has been made. Therefore, this staging PET/CT is not performed in radiotherapy position. A *staging* PET/CT is usually performed on a soft curved table top, while *treatment planning* scans are performed on a hard, rigid, flat radiotherapy table top, identical to the radiotherapy setting. The position of the patient during a staging PET/CT is optimised for both patient comfort and image quality, e.g. with a cushioned head rest and with the arms elevated, to prevent thorax imaging artefacts by beam hardening and truncation. Patient-positioning during treatment planning PET/CT is optimised for reproducibility and radiation-beam arrangement avoiding dose in body parts not belonging to the target volume, e.g. arms in thoracic tumours. Therefore, rigid transformations cannot fully compensate for the patient position differences. Software to deformably register staging PET/CTs

with a planning-CT is currently commercially available and shows potential improvement in alignment, even in case of preoperative PET/CT with a postoperative CT [17–22]. The staging PET, however, can only be used for radiotherapy planning when performed shortly before start of radiotherapy. This is a pre-requisite to prevent disease progression in the meantime, resulting in understaging and undertreatment of the disease [23, 24].

1.3.4 Motion

Patient movement complicates accurate co-registration between the PET and the CTAC, and between the PET(/CT) and the planning-CT, with the above-described consequences. The effect on attenuation and thereby scatter correction, will especially be large in moving tumours at the interface of two types of tissue with large differences in Hounsfield units (photon attenuation), for example, the lower part of the lung and the liver dome around the diaphragm [25]. Motion also negatively influences the PET-image, when occurring during the relatively lengthy PET-acquisition itself, since it causes image-blurring, i.e. an overestimation of the volume of pathological radiopharmaceutical uptake and an underestimation of the concentration of radiopharmaceutical.

1.3.4.1 Types of Motion

Motion can be divided into external patient motion (e.g. rotation of the head, opening of the jaw) or internal target motion (e.g. bladder filling, diaphragm motion during breathing, bowel motion).

External patient motion is mostly non-repetitive and effectuated by skeletal muscles innervated by the somatic nervous system. It can be *bulky*, for example, when the whole body or a full extremity is moved, which can be minimised using fixation devices and patient instruction. External patient motion can be more challenging in patients who are not able to cooperate in minimising motion, e.g. very young patients, patients with reduced mental capacities, who may require sedation. External patient motion can also be *compact* such as uncontrollable tremor as a result of, e.g. Parkinson's disease.

Internal target motion is mostly involuntary, *periodic* or oscillatory in nature and is caused by autonomic (mainly sympathetic) nerve innervation of effector muscles, such as the myocardium and respiratory muscles, including the diaphragm. *Aperiodic* involuntary internal target motion, such as bowel motion, bladder filling or, at least partly, eye movement, should also be taken into account. Most forms of internal target motion are unpreventable and require special measures to deal with.

Methods to compensate for motion during the PET-acquisition will be highlighted here. Methods to compensate during the radiotherapy fraction itself are outlined elsewhere.

1.3.4.2 Motion Correction Methods

Alignment

Minimising spatial mismatch *between* scans and irradiation is achieved by performing all image acquisitions and the treatment in highly similar (i.e. reproducible), position (preferably radiotherapy position), with respect to the internal coordinate system (isocentre) of the scanners and treatment gantry. Accurate alignment can be achieved with the help of external lasers and skin (tattoo) markers. To prevent deformations, immobilising devices can be helpful. These immobilising devices can be *personalised*, for example, thermoplastics masks, bite blocks, and some headrests, or *generic*, such as overlay beds, bands, strap restraints, sand bags, shoulder depressors, head clamps, etc. Evaluation of the position directly before the start of a radiotherapy fraction and directly afterwards can be achieved by online imaging, where the 2D or 3D generated radiographic images, optional including fiducial markers, are compared with the planning-CT and its 2D digital reconstructed radiographs [26].

Minimising patient motion *during* acquisition can largely be achieved by clear patient instructions, starting with an understandable explanation of the importance of motionlessness. Moreover, immobilising devices could improve the compliance. Patients with postural pain despite adequate analgesia may be helped with reduced acquisition time, which can be compensated for with higher injected dose of the radiopharmaceutical to avoid deterioration of image quality (generally: halving acquisition time requires doubling the radiopharmaceutical dose). Alternatively, unconventional positioning can be attempted, but this will severely hamper the use of these images for radiotherapy planning. When the target volume is located near the bladder or urethra, for example, in rectum or cervix carcinoma, spatial mismatch can arise between the PET and CT, due to bladder filling between both acquisitions. For this purpose, imaging is generally performed directly after voiding and the CTAC is acquired craniocaudally followed by the PET caudocranially, to keep the time interval between PET and CT in the pelvic area as short as possible. In very anxious patients, benzodiazepines can be prescribed or even sedatives can be administered.

Respiratory motion-induced interplay effects contribute most to intra-acquisitional and intrafractional motion of breast, lung, liver and pancreatic tumours, due to the period of normal breathing (2–5 s/ breath) with respect to the duration of PET-acquisition (2–5 min per bed position) or a therapeutic fraction (20–40 s per beam angle) [27]. The contemporary methods to compensate for respiratory motion will therefore be discussed separately in the next paragraph.

Compensation Methods for Respiratory Motion

Methods to control respiratory motion can be divided into four motion-encompassing categories. The first category exists of external compression methods, such as the abdominal compression technique, where an external device applies pressure on the abdomen, to minimise motion in the diaphragm. These methods are especially useful for tumours close to the diaphragm, e.g. liver dome and lower lung lobes [28].

The second category contains *controlled breathing methods*, i.e. instead of free breathing, instructions are provided to the patient to hold their breath on a specific

moment in the respiratory cycle or to force shallow breathing. An automatic breath control device, used in the active breathing control-technique, can also be used to regulate the respiratory cycle.

By *respiratory gating*, being the third motion-encompassing category, the respiratory cycle is measured. The longest period in the respiratory cycle where the least thoracic volume changes occur is determined and the corresponding frames in the list-mode acquired PET-data are used for reconstruction, resulting in a ‘frozen image’. This gating method generally requires longer acquisition of thorax and upper abdomen bed positions, since only a part of the acquired data is used for image reconstruction, making it a lossy technique. Newer techniques are able to only acquire PET-data at the usable moments in the respiratory cycle.

The last motion-encompassing method uses the PET-data itself for gating purposes and, therefore, requires no additional hardware. *Data-driven gating* defines an optimal binning strategy by principle component analysis. It encompasses the elastic deformation of the images post-acquisition. With this technique all acquired data are used during image reconstruction and it is, therefore, called a lossless technique [29]. Correction of lesion-specific motion seems possible by the positron emission particle tracking technique combined with time of flight information, but its clinical added value currently still needs to be determined [30].

One should keep in mind that the result of motion mitigation used for PET should match that of either CTAC and treatment-CT to prevent spatial functional-anatomical mismatch with all earlier mentioned disadvantages. Apart from the technical possibilities, one should consider the clinical value of motion compensation. When no motion compensation will be applied during the delivery of radiotherapy, motion correction during PET/CT- and treatment planning-CT-acquisition might be undesired. Therefore, some institutions use the ungated CT images for treatment planning. Using magnetic resonance-based linear accelerator for radiotherapy, intrafractional adjustment of the treatment plan to motion is possible (Chaps. 6 and 7).

1.4 Target Volume Delineation

1.4.1 PET/CT in Target Volume Delineation

Adding biological PET/CT-information, sometimes addressed to as biological or metabolic target volume, to the planning-CT could be helpful to clarify the nature (benign versus malignant) of a tumour difficult to differentiate on solely CT. It is assumed that in some tumour or scenarios tumour borders can be defined more sharply, by more clearly differentiating malignant from non-malignant tissue (e.g. post-obstructive atelectasis), by distinguishing ambiguous lymph nodes, and by differentiating residual or recurrent disease from post-treatment scar tissue [31–33]. The addition of PET/CT in TVD has shown to lower interobserver variability in several disease sites, compared to CT-based delineation [34–37]. The added value of PET/CT target volume delineation depends on, e.g., the applied segmentation

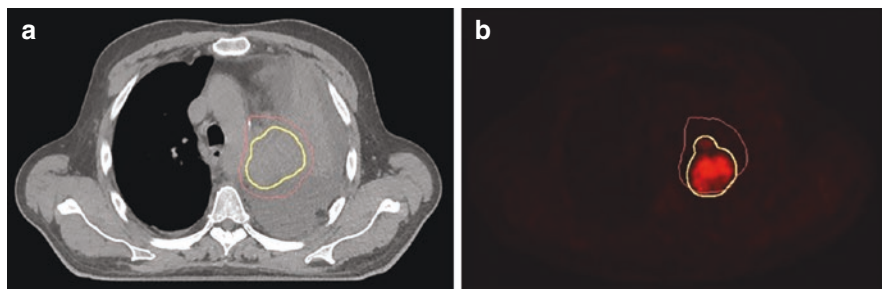


Fig. 1.3 (a) The target volume (GTV based on CT in yellow and CTV in red) in a non-small cell lung cancer patient delineated on CT only, (b) the target volume delineated with the additional information of [^{18}F]FDG PET/CT (GTV based on PET in yellow, same CTV in red)

technique and tumour location and type, which will be discussed in the following sections. In the remainder of this chapter, the PET(/CT)- and planning-CT-based target volumes are referred to as PET-TV and CT-TV, respectively. A comparison between a PET-TV and a CT-TV is provided in Fig. 1.3.

1.4.2 PET/CT Segmentation Methods

1.4.2.1 Manual, Semi-Automatic and Automatic Segmentation Methods

The contoured target volumes depend on the used segmentation method, which classifies the voxels of an image as either being malignant or non-malignant [38]. There are multiple segmentation methods under development, with different levels of complexity and intuitiveness.

Manual tumour segmentation, still most common in clinical practice, is based on visual inspection of the spatial [^{18}F]FDG-distribution, combined with the available anatomical information. This method requires interpretation, which makes it extremely prone to observer variability. Standardised instructions are therefore desired. Recommendations are given in head and neck squamous cell carcinoma (HNSCC) by Lee et al. [39] and Schinagl et al. [40].

However, since radiation treatment planning is still based on anatomical CT-imaging, PET ought to be seen as additional source of information on the GTV, not as a replacement of CT.

As PET is a quantitative imaging modality, alternative (*semi*)*automatic tumour segmentation* approaches have been developed which have shown to be more reproducible than manual delineation. Those methods are described next.

Thresholding is, after manual delineation, the most applied and intuitive approach in clinical practice. Multiple techniques have been proposed to determine the optimal threshold intensity value of a quantitative PET-parameter to discern benign from malignant voxels. The most often used semi-quantitative PET-parameter is the standardised uptake value (SUV). This is the activity-concentration in a voxel (in

Bq/mL) normalised for administered activity of the radiopharmaceutical per unit patient bodyweight (in Bq/g). This threshold can be set as an absolute threshold (e.g. $SUV \geq 2.5$ g/ml) or related to the mean, peak or maximum intensity in the lesion (e.g. $SUV \geq 50\% \cdot SUV_{\max}$). Alternatively, an internal reference is used, such as the lesion-to-background ratio. It is likely that the optimal threshold value depends on tumour location (background, movement) and tumour size (with respect to PET-scanner resolution). A clear outline of multiple threshold value formulas is provided by Zaidi et al. [41].

A less intuitive category of segmentation methods, *variational methods*, is based on spatial intensity variation between the foreground and the background. Examples are edge and ridge detection methods, such as Sobel operators and Watershed transformations, or active contouring methods. Drever et al. [42] provide a comprehensive comparison between the Sober, Watershed and thresholding approaches for PET TVD. An active contouring method, better known as a snake, is a spline, a function defined by multiple polynomial sub-functions, which incorporates prior knowledge, e.g. smoothness and shape, to deform around the object. Active contouring makes subpixel contouring possible [43, 44]. These variational segmentation methods are complicated due to their sensitivity to image noise, especially in case of gradient-based methods and when the lesion is surrounded by metabolic active areas [15, 45, 46].

Segmentation can also be performed by a *pattern recognition learning approach*, also known as machine learning. A distinction should be made between *classification* in case of supervised learning on the one hand, i.e. when the nature (benign vs malignant) of each voxel is known, and *clustering* by unsupervised learning on the other hand. Both techniques are based on the extraction of features from the image. Classification is widely applied in other imaging modalities, but may be hampered in PET by the large heterogeneity in tumour uptake. Clustering, on the contrary, seems valuable in target segmentation in PET. The most simple and common clustering method is the k-means-algorithm, encompassing a ‘hard’ boundary that includes every voxel in one of the two clusters, ‘tumour’ or ‘no tumour’. The centres of the clusters are initialised and updated during the algorithm, until the final clustering is retrieved. The boundaries can also be soft, allowing uncertain voxels to be probabilistic part of both clusters, which is synonymised as fuzzy. Examples of these soft boundary clustering methods are fuzzy k-means or fuzzy C-means algorithms. These computational complex learning methods, especially supervised learning, can provide much flexibility, but can also be challenging and counterintuitive [39, 47].

Within the increasingly popular field of radiomics, a large number of imaging features are extracted, which may contribute to the TVD, especially in learning segmentation [48–50]. By using a deep learning approach, features can be extracted automatically. Huang et al. [51] and Guo et al. [52] contoured the GTV of HNSCC patients on PET/CT-images accurately and with high efficiency with a deep neural network, compared to more conventional segmentation methods. The gold standard was considered manual contouring.

The last category of segmentation methods, *statistical image segmentation*, differentiates between tumour uptake and surrounding tissue by probabilistic

calculation and estimation of the data. This stochastic modelling approach deals well with high noise PET-data, but is at risk of local optimal solutions in the optimisation. An example is the Gaussian mixture model, which handles the intensities as independent and Gaussian distributed. This dependency is not necessary in the usage of hidden Markov models, another statistical segmentation method [53]. Hatt et al. [54, 55] improved the segmentation of small and/or heterogeneous lesions with the statistical segmentation algorithm fuzzy locally adaptive Bayesian.

Shepherd et al. [56] performed a double-blind comparative study for 30 different and combined segmentation techniques in 2012, from manual to full automatic and concluded that up to then, manual segmentation outperformed all the (semi-)automatic delineation methods in highest overall accuracy. An overview of the PET-segmentation methods can be found in Zaidi et al. [41] and Hatt et al. [54].

1.4.2.2 Drawback of Segmentation Methods

Although manual segmentation is still most commonly performed in clinical practice, it shows a higher interobserver variability than the application of (semi-) automatic segmentation methods [41]. The accuracy of manual segmentation depends on the experience and expertise of the observer and proposes the risk of observer overrating. Rasch et al. [57] showed that updating the PET-TV defined by the treating physician with the assessment of 5–7 radiation oncologists and a radiologist leads to an alteration in 45% of the cases. Manual delineation and especially in agreement of multiple experts, preferably both radiation oncologists and medical imaging specialists, is labour-intensive and hardly feasible in current high demanding-high throughput oncology healthcare. Therefore, the development of a reliable automatic PET segmentation method (PET-AS) is desired. Automatic segmentation of PET-only data is currently under development, although automatic PET segmentation with CT-data outperforms automatic PET-only segmentation, with the disadvantage of increased complexity. For application of PET-AS, the algorithms should be accurate and precise under different clinical circumstances. Unfortunately, none of the currently existing algorithms fulfils all needs [48].

1.4.2.3 Consensus Algorithms

The success of multiple segmentation algorithms is strived to be combined by two new methods: the Majority Vote and Simultaneous Truth And Performance Level Estimate (STAPLE) method with their variances. The first method decides whether a voxel is included in the target volume, based on the outcome of the majority of the methods. The latter estimates the segmentation result, based on a probability distribution function of multiple separate segmentation methods and their performance [58]. McGurk et al. [59] compared both consensus methods in five (semi-) automatic PET segmentation algorithms and concluded that both Majority Vote and STAPLE were robust and more accurate for all separate segmentation methods in different experimental circumstances. Schaefer et al. [60] and Dewalle-Vignion et al. [61] confirmed these findings, the latter for STAPLE in semi-clinical setting, including comparison with manual segmentation.

Berthon et al. [62] developed a third consensus method: the supervised machine learning algorithm Automatic decision Tree-based Learning Algorithm for Advanced Segmentation (ATLAAS), which includes a decision tree model to select the most appropriate of 9 automatic segmentation methods, instead of combining the results like the earlier described consensus methods. ATLAAS proved robust segmentation with higher accuracy compared to each of the individual segmentation methods in phantom setting and showed promising clinical results in HNSCC PET tumour segmentation [62, 63].

For now, the International Atomic Energy Agency expert report, published in 2009 and updated for non-small cell lung carcinoma (NSCLC) in 2019, recommends that target volumes, delineated by a PET-AS technique, as part of standard care, should always be visually checked by an experienced observer [64].

1.4.3 Disease Sites

1.4.3.1 NSCLC and SCLC

Several studies investigated the beneficial effect of PET(/CT) on TVD. Most evidence is available in non-small cell and small cell lung cancer (NSCLC and SCLC), for which Hallqvist et al. [65] performed a systematic review of the role of PET/CT in treatment planning. Their review shows a significant change in PET-TV, compared to CT-TV in approximately 40% of NSCLC patients. Moreover, in 20% of the patients, the intent of the treatment was changed from radical high-dose to palliative low-dose radiotherapy, as a result of upstaging of the tumour. In SCLC, target volume changed in 20% and treatment intention changed in 10% of the cases, when PET is added to the TVD [65]. For both, NSCLC and SCLC, [¹⁸F]FDG PET guides the primary tumour contour, in particular in case of atelectasis, even though the tumour boundaries are drawn on the planning-CT in lung window-width/window-level setting. The PET-TV results are only applicable for target volumes defined on PET/CT-images in radiotherapy position, as discussed in ‘Technical aspects’ and independent of the presence of a staging PET/CT.

De Ruyscher et al. [66] compared PET-TVs with CT-TVs in mediastinal lymph nodes in a treatment planning study and subsequently treated all included NSCLC patients according to the PET-delineated treatment plan in a single-arm prospective clinical trial. The results obtained using the 3D-technique employed at the time showed a low isolated lymph node recurrence rate of 2.3%. Bradley et al. [32] published their findings of the Radiation Therapy Oncology Group study in NSCLC patients. They showed a disagreement of 51% comparing nodal PET-TV with CT-TV, mostly caused by the in- or exclusion of one or two nodal stations. Also in this study, all patients received irradiation according to the PET/CT derived treatment plan. In 2% of the patients, i.e. 1 out of 46 patients, failure occurred in [¹⁸F]FDG-negative lymph nodes, not included in the PET-TV, which is stated in this study as quite low. In 2018, the MAASTRO group investigated the validity of [¹⁸F]FDG PET-based selective nodal irradiation in the era of Intensity-modulated radiation therapy [67]. They, again, reported on an isolated nodal failure rate of 2.3%. So, since elective nodal irradiation is associated

with lower achievable doses and higher side-effects, selective nodal irradiation is to be regarded the standard, also in the era of high conformal irradiation techniques.

In SCLC, again the MAASTRO group published their findings on 60 SCLC patients with limited disease SCLC [68]. They reported on an isolated nodal failure rate of 3%, mainly in the supraclavicular fossa. The selective nodal approach, based on [¹⁸F]FDG PET/CT, was subsequently employed in the CONVERT trial, showing no detrimental effects on regional control [69].

The systematic review and meta-analysis of Hallqvist et al. [65] on [¹⁸F]FDG PET in NSCLC included no studies with level I evidence, but nonetheless concluded that ‘PET/CT for dose planning improves target definition and patient selection’ in NSCLC patients. Only in 2020, the PET-PLAN results were published, underlining the results of the meta-analysis as well as recommendations by European Committees (see below). Nestle et al. [70] randomly assigned 205 patients with inoperable advanced stage NSCLC to PET/CT-based target volume including elective nodal irradiation versus PET-based treatment planning, including selective nodal irradiation only. At a follow-up time of 29 months at median, the locoregional progression rate of the [¹⁸F]FDG PET-based group was non-inferior, and in fact even lower than that for the conventional target group anticipated in the protocol, and also the toxicity was non-inferior. Thus, the recommendation by the European Organisation for Research and Treatment of Cancer (EORTC) in 2017, that PET/CT is standard for treatment planning in lung cancer holds true, as do the guidelines adopted by the European Society for Radiotherapy and Oncology Advisory Committee in Radiation Oncology Practice (ESTRO) guidelines in 2018 [71], and the Joint EANM/SNMMI/ESTRO practice recommendations for the use of 2-[¹⁸F]FDG PET/CT external beam radiation treatment planning in lung cancer V1.0, which was published in March 2022 [72].

1.4.3.2 HNSCC

In HNSCC, various publications have shown the PET-TV to be smaller than those derived by CT or even MRI, when compared to histopathological resection specimens [73–80]. However, since the tumours originate from the oral mucosa and may exhibit superficial tumour spreading not visible on macroscopic imaging, the value of a thorough clinical examination is still high. Therefore, treatment planning solely based on [¹⁸F]FDG PET/CT is still not standard of care.

Although Delouya et al. [75] and Chatterjee et al. [81] did not show significant changes in nodal target volume comparing PET-TV with CT-TV, Ciernik et al. [78] showed target volume changes up to approximately 20%, based on the comparison in six patients. Bearing in mind the high incidence of false-positive readings due to reactive lymph nodes in the head and neck region, though, the [¹⁸F]FDG PET finding should always carefully be compared to that of the anatomical imaging modality, albeit CT or MRI [82, 83]. Instead, dose de-escalation based on the [¹⁸F]FDG PET and CT finding may be investigated, which is at present the objective of a phase II clinical trial [84–86].

In HNSCC, several guidelines recommend the application of [¹⁸F]FDG PET in TVD, including those of the National Comprehensive Cancer Network and the International Atomic Energy Agency [87].

1.4.3.3 Oesophageal Cancer

In a prospective study in oesophageal cancer patients, Ng et al. [88] included [^{18}F]FDG-avid disease, not identified by CT, in the PET-TV in 76% of 38 cases. This changed the intent of the treatment from curative to palliative in 24% of 57 cases. Apolle et al. [89] compared the GTV based on [^{18}F]FDG PET with that defined by fiducial markers implanted at the proximal and distal side of the tumour. They concluded that the marker locations corresponded reasonably well with metabolic tumour edges (mean: 5.4 mm more distally). The delineation of the gross nodal volume may substantially change using [^{18}F]FDG PET, as illustrated by Jimenez-Jimenez et al. [90]. The use of PET/CT in the staging and planning of radio(chemo)therapy seems to improve local recurrence-free survival in oesophageal cancer [91]. The value of [^{18}F]FDG PET in oesophageal cancer has recently been extensively reviewed [92, 93].

1.4.3.4 Gynaecological Tumours

In gynaecological oncology, the primary tumour, e.g. of the cervix, is visualised under clinical examination as well as by MRI (mainly T2-weighted imaging). MRI is used for primary staging as well as for brachytherapy planning [94, 95]. However, the value of [^{18}F]FDG PET for diagnosis and radiation treatment planning, mainly in terms of defining the nodal TV, is becoming increasingly apparent [77, 78, 88, 90, 96–99].

1.4.3.5 Lymphoma

The use of [^{18}F]FDG PET/CT for treatment response monitoring and target volume delineation in both, Hodgkin's lymphoma and non-Hodgkin's lymphoma, is unequivocally highly recommended, as described by the International Lymphoma Radiation Oncology Group [77, 100–104].

1.4.3.6 Other Tumours

The use of [^{18}F]FDG-PET/CT for TVD in case of primary brain tumours or prostate cancer is not beneficial. Tracers enabling visualisation and delineation of those solid tumours are discussed in Chap. 2.

It should be kept in mind that the success of PET TVD for nodal contouring depends on its sensitivity and specificity [66, 78, 97]. For regional lymph node detection, a high specificity between 0.90 (NSCLC) and 0.97 (cervical cancer) is typically observed, versus a moderate sensitivity between 0.66 (oesophageal cancer) and 0.84 (HNSCC) [83, 105–110].

1.5 Cons and Pitfalls

In the previous sections, the added value of PET in treatment planning is summarised. There are, however, some considerations that should be kept in mind when applying this technique.

1.5.1 Limited Spatial Resolution and High Signal-to-Noise Ratio of PET

When using PET-imaging for TVD, one must be aware of the technical shortcomings of PET in general, which is shortly discussed in section ‘Technical aspects’. PET is restricted by a limited spatial resolution of around 3–5 mm full-width-at-half-maximum. Due to this low spatial resolution compared to anatomical modalities such as CT and MRI, small lesions will be underestimated in activity concentration or might even be missed (i.e. false-negative), due to the resulting partial volume effects. The consequences of this effect should be considered in all small, low contrast lesions (typically <2 cm) and depend, amongst others, on the resolution of the PET/CT-scanner, the applied reconstruction algorithm, the post-reconstruction filter and the shape, size, uptake and motion of the lesion [111]. Additional post processing and/or resolution modelling reconstruction algorithms can be applied to correct for partial volume effects up to a certain extent, although the risk of introducing new artefacts should be considered [54].

PET/CT-images can have a low signal-to-noise ratio, dependent of patient- and institution-specific factors. The signal-to-noise ratio is, amongst others, negatively influenced in case of limited radiopharmaceutical uptake, when the injected dose of the radiopharmaceutical is not adjusted to acquisition time (e.g. lossy respiratory gating) or in case of large patient attenuation (high body mass index). The latter might cause lesions to go undetected or treatment planning to become less reproducible. On the contrary, the signal-to-noise ratio is enhanced by improved system geometry (longer bores, whole-body PET-scanners), advanced (digital) detectors and improved reconstruction algorithms (time-of-flight, Bayesian methods, deep learning methods, smaller voxel sizes) [112, 113].

1.5.2 Interpretation Errors Due to Limited Specificity (and Sensitivity) of the Radiopharmaceutical [¹⁸F]FDG

Although regions with high [¹⁸F]FDG-uptake represent tissues with high glucose-demand, the amount of uptake does not fully depend on the presence and the degree of malignancy. High physiological uptake in healthy tissue or low uptake in tumour tissue can be physiological (e.g. brain, liver, urinary tract) or occur by improper patient preparation (hyperglycaemia, hyperinsulinemia, some drugs, brown adipose tissue). False-positive lesions can be found on PET/CT-images due to influx of inflammatory cells (lymphocytes, macrophages), due to infection (e.g. pneumonia), inflammatory conditions (e.g. sarcoidosis) or after invasive intervention (e.g. biopsy, radiotherapy). Another frequent cause of false-positive lesions are benign lesions such as incidentalomas in the thyroid or intestines, that are misinterpreted as metastases or secondary primaries and often require additional (invasive) diagnostics, potentially leading to unnecessary delay in definite treatment.

The success of lesion detection using [^{18}F]FDG depends on the metabolic profile of the tumour histology as some subtypes are notoriously false-negative (e.g. low-grade tumours such as most neuroendocrine tumours and low-risk prostate cancer or those with much extracellular matrix such as mucinous adenocarcinomas) and its location (i.e. in regions with physiological high background including brain, liver, kidneys and bladder) are other influencing factors. Therefore, the disease-specific sensitivity and specificity of the radiopharmaceutical should be considered. The additional value of PET in nodal delineation is presumably caused by the inclusion or exclusion of nodal stations, which depends on the error rate. PET's high sensitivity is especially useful in the inclusion of nodal stations in the GTV.

Altogether, it can be stated that lesions for treatment planning should ideally be interpreted jointly by an experienced nuclear medicine physician and radiation oncologist to place the images into context and to minimise the consequences of false-positive or -negative findings [66]. In case of doubt, it is recommended to obtain cytological or histopathological confirmation. This is especially of importance when treatment would change from curative- to palliative intent, due to distant metastases detected by PET.

1.6 Future Outlook

Radiation treatment outcome may be improved by incorporating patient-specific tumour control probability and normal tissue complication probability in the treatment plan, based on [^{18}F]FDG-derived biological information of the tumour and the OAR.

[^{18}F]FDG uptake in lesions, to some extent, reflects sensitivity of the tumour to treatment. Less radiosensitive areas may profit from treatment intensification, e.g. hypoxia modifiers, immunotherapy, or radiation dose escalation. Personalised dose escalation may be beneficial in selected patients (stratification) and/or tumour subvolumes (subvolume boosting, dose painting by contours), even on voxel level (dose painting by numbers).

To study feasibility, toxicity and efficacy of dose escalation in stage III NSCLC patients, the PET-boost trial was initiated in 2010. In this multicentre randomised phase II clinical trial, hypofractionated dose escalation was prospectively studied in both the entire primary tumour (arm A) as in subvolumes of the GTV, defined by increased [^{18}F]FDG uptake (arm B). First, a planning study reported by van Elmpt et al. [114] demonstrated feasibility of dose escalation, both in the entire primary tumour (arm A) as well as in subvolumes of the GTV (arm B). Subsequently, toxicity was tested. Preliminary results are reported by van Diessen et al. [115]. Although increased acute and long-term toxicities were observed in the study, the dose limits of the OAR were maintained. Efficacy results were presented on the World Conference on Lung Cancer 2020 (which took place virtually in January 2021). An excellent local control rate was observed in both hypofractionated dose escalation arms, with a 2-year local failure rate of less than 20% and a regional failure of only 27% [116]. Final results are awaited.

Additional research is required into mechanisms of radioresistance, methods (radiopharmaceuticals, parameters) to adequately quantify radiosensitivity and on techniques to accurately deliver the biologically adapted dose to the patient. The relation between the imaging parameter and dose escalation should also be studied, as well as the necessity of dose escalation (prescription function) [117].

Pre-treatment [¹⁸F]FDG PET/CT also provides plenty of information on the surrounding tissue. This information might be useful in predicting toxicity in the surrounding OAR, although limited studies are available yet. Van Dijk et al. [118] showed that pre-treatment high metabolic parotid gland activity is associated with lower risk of developing late xerostomia. Anthony et al. [119] demonstrated that pre-treatment [¹⁸F]FDG uptake in combination with CT lung texture features in low-, medium-, and high-dose regions, could predict the risk of radiation pneumonitis in lung cancer patients. Zschaecck et al. showed that [¹⁸F]FDG PET uptake in normal tissue within irradiated HNSCC [120] and oesophageal cancer [121] during treatment is a prognostic factor for local tumour control. Besides these promising studies, more research should be performed to analyse whether [¹⁸F]FDG PET image biomarkers (i.e. radiomics) of non-tumorous tissue have predictive potential. The result of van Dijk et al. [118] should be verified in an independent dataset. To verify the findings of Anthony et al. [118], a larger patient population, in varying circumstances, with more positive cases is required.

When the biological information provided by PET/CT of both the tumour and the non-tumorous tissue is integrated in the treatment plan, this may result in a more personalised treatment plan with maximal tumour control probability and minimal normal tissue complication probability.

Acknowledgements We would like to thank dr. C.S. van der Vos for her valuable input, Mr. G. Kracht for the design of Fig. 1.1 and prof. dr. E.G.C. Troost for writing the paragraph on the clinical value of [¹⁸F]FDG PET for various tumour sites and for providing Fig. 1.3.

References

1. Chua S. PET/CT in radiotherapy planning. In: Chua S, editor. PET/CT. 1st ed. Berlin: Springer International Publishing; 2017. 78p.
2. International Commission on Radiation UaM. ICRU report 50: prescribing, recording and reporting photon beam therapy 1993;os-26(1):3–38.
3. Winter RM, Leibfarth S, Schmidt H, Zwirner K, Monnich D, Welz S, et al. Assessment of image quality of a radiotherapy-specific hardware solution for PET/MRI in head and neck cancer patients. *Radiother Oncol.* 2018;128(3):485–91.
4. Thorwarth D, Leibfarth S, Monnich D. Potential role of PET/MRI in radiotherapy treatment planning. *Clin Transl Imaging.* 2013;1(1):45–51.
5. Paulus DH, Thorwarth D, Schmidt H, Quick HH. Towards integration of PET/MR hybrid imaging into radiation therapy treatment planning. *Med Phys.* 2014;41(7):072505.
6. van Sluis J, de Jong J, Schaar J, Noordzij W, van Snick P, Dierckx R, Borra R, Willemsen A, Boellaard R. Performance characteristics of the digital biograph vision PET/CT system. *J Nucl Med.* 2019;60(7):1031–6.

7. van der Born D, Pees A, Poot AJ, Orru RVA, Windhorst AD, Vugts DJ. Fluorine-18 labelled building blocks for PET tracer synthesis. *Chem Soc Rev.* 2017;46(15):4709–73.
8. Conti M, Eriksson L. Physics of pure and non-pure positron emitters for PET: a review and a discussion. *EJNMMI Phys.* 2016;3(1):8.
9. Vander Heiden MG, Cantley LC, Thompson CB. Understanding the Warburg effect: the metabolic requirements of cell proliferation. *Science.* 2009;324(5930):1029–33.
10. Boellaard R, Delgado-Bolton R, Oyen WJ, Giammarile F, Tatsch K, Eschner W, et al. FDG PET/CT: EANM procedure guidelines for tumour imaging: version 2.0. *Eur J Nucl Med Mol Imaging.* 2015;42(2):328–54.
11. Boellaard R, Willemsen AT, Arends B, Visser EP. EARL procedure for assessing PET/CT system specific patient FDG activity preparations for quantitative FDG PET/CT studies. 2014.
12. Cherry SR, Dahlbom M. PET: physics, instrumentation, and scanners. In: Phelps ME, editor. *PET: physics, instrumentation, and scanners.* New York, NY: Springer; 2006. p. 1–117.
13. Cherry SR, Sorenson JA, Phelps ME. *Physics in nuclear medicine.* Philadelphia: Elsevier Saunders; 2012.
14. Paulino AC. *PET-CT in radiotherapy treatment planning.* Amsterdam: Elsevier Health Sciences; 2008.
15. Greco C, Rosenzweig K, Cascini GL, Tamburrini O. Current status of PET/CT for tumour volume definition in radiotherapy treatment planning for non-small cell lung cancer (NSCLC). *Lung Cancer.* 2007;57(2):125–34.
16. van de TA W, van JA D. PET-CT in radiation treatment planning. In: Database R, editor. *Federatie medisch specialisten. Kloosterhof Neer Bv, Netherlands;* 2016. p. 716–49. <https://libris.nl/BookInfo/GetSample?guid=6df17221-0444-4ee0-b691-c84be878a2d2>. https://richtlijndatabase.nl/gerelateerde_documenten/f/17305/PET-CT%20in%20Radiation%20Treatment%20Planning.pdf
17. Kovalchuk N, Jalisi S, Subramaniam RM, Truong MT. Deformable registration of preoperative PET/CT with postoperative radiation therapy planning CT in head and neck cancer. *Radiographics.* 2012;32(5):1329–41.
18. Fortin D, Basran PS, Berrang T, Peterson D, Wai ES. Deformable versus rigid registration of PET/CT images for radiation treatment planning of head and neck and lung cancer patients: a retrospective dosimetric comparison. *Radiat Oncol.* 2014;9:50.
19. Guo Y, Li J, Zhang P, Shao Q, Xu M, Li Y. Comparative evaluation of target volumes defined by deformable and rigid registration of diagnostic PET/CT to planning CT in primary esophageal cancer. *Medicine (Baltimore).* 2017;96(1):e5528.
20. Hanna GG, De Koste JRVS, Carson KJ, O'Sullivan JM, Hounsell AR, Senan S. Conventional 3D staging PET/CT in CT simulation for lung cancer: impact of rigid and deformable target volume alignments for radiotherapy treatment planning. *Br J Radiol.* 2011;84(1006):919–29.
21. Hwang AB, Bacharach SL, Yom SS, Weinberg VK, Quivey JM, Franc BL, et al. Can positron emission tomography (PET) or PET/computed tomography (CT) acquired in a nontreatment position be accurately registered to a head-and-neck radiotherapy planning CT? *Int J Radiat Oncol Biol Phys.* 2009;73(2):578–84.
22. Ward G, Ramasamy S, Sykes JR, Prestwich R, Chowdhury F, Scarsbrook A, et al. Superiority of deformable image co-registration in the integration of diagnostic positron emission tomography-computed tomography to the radiotherapy treatment planning pathway for oesophageal carcinoma. *Clin Oncol (R Coll Radiol).* 2016;28(10):655–62.
23. Konert T, Vogel W, MacManus MP, Nestle U, Belderbos J, Gregoire V, et al. PET/CT imaging for target volume delineation in curative intent radiotherapy of non-small cell lung cancer: IAEA consensus report 2014. *Radiother Oncol.* 2015;116(1):27–34.
24. Everitt S, Plumridge N, Herschtal A, Bressel M, Ball D, Callahan J, et al. The impact of time between staging PET/CT and definitive chemo-radiation on target volumes and survival in patients with non-small cell lung cancer. *Radiother Oncol.* 2013;106(3):288–91.
25. Fin L, Daouk J, Morvan J, Bailly P, El Esper I, Saidi L, et al. Initial clinical results for breath-hold CT-based processing of respiratory-gated PET acquisitions. *Eur J Nucl Med Mol Imaging.* 2008;35(11):1971–80.
26. Goyal S, Kataria T. Image guidance in radiation therapy: techniques and applications. *Radiol Res Pract.* 2014;2014:705604.

27. Langen KM, Jones DTL. Organ motion and its management. *Int J Radiat Oncol*. 2001;50(1):265–78.
28. Huang TC, Wang YC, Chiou YR, Kao CH. Respiratory motion reduction in PET/CT using abdominal compression for lung cancer patients. *PLoS One*. 2014;9(5):e98033.
29. Kesner AL, Meier JG, Burckhardt DD, Schwartz J, Lynch DA. Data-driven optimal binning for respiratory motion management in PET. *Med Phys*. 2018;45(1):277–86.
30. Tumpa TR, Acuff SN, Gregor J, Lee S, Hu D, Osborne DR. Respiratory motion correction using a novel positron emission particle tracking technique: a framework towards individual lesion-based motion correction. *Conf Proc IEEE Eng Med Biol Soc*. 2018;2018:5249–52.
31. Schechter NR, Gillenwater AM, Buyers RM, Garden AS, Morrison WH, Nguyen LN, et al. Can positron emission tomography improve the quality of care for head-and-neck cancer patients? *Int J Radiat Oncol Biol Phys*. 2001;51(1):4–9.
32. Bradley J, Bae K, Choi N, Forster K, Siegel BA, Brunetti J, et al. A phase II comparative study of gross tumor volume definition with or without PET/CT fusion in dosimetric planning for non-small-cell lung cancer (NSCLC): primary analysis of radiation therapy oncology group (RTOG) 0515. *Int J Radiat Oncol Biol Phys*. 2012;82(1):435–41.e1.
33. Yaraghi Y, Jabbari I, Akhavan A, Ghaffarian P, Monadi S, Saeb M. Comparison of PET/CT and CT-based tumor delineation and its effects on the radiation treatment planning for non-small cell lung cancer. *Iran J Nucl Med*. 2018;26(1):9–15.
34. Anderson CM, Sun W, Buatti JM, Maley JE, Policeni B, Mott SL, et al. Interobserver and intermodality variability in GTV delineation on simulation CT, FDG-PET, and MR images of head and neck cancer. *J Radiat Oncol*. 2014;1(1):006.
35. Metwally H, Courbon F, David I, Filleron T, Blouet A, Rives M, et al. Coregistration of prechemotherapy PET-CT for planning pediatric Hodgkin's disease radiotherapy significantly diminishes interobserver variability of clinical target volume definition. *Int J Radiat Oncol*Biol*Phys*. 2011;80(3):793–9.
36. Buijsen J, van den Bogaard J, van der Weide H, Engelsman S, van Stiphout R, Janssen M, et al. FDG-PET-CT reduces the interobserver variability in rectal tumor delineation. *Radiother Oncol*. 2012;102(3):371–6.
37. van Baardwijk A, Bosmans G, Boersma L, Buijsen J, Wanders S, Hochstenbag M, et al. PET-CT-based auto-contouring in non-small-cell lung cancer correlates with pathology and reduces interobserver variability in the delineation of the primary tumor and involved nodal volumes. *Int J Radiat Oncol Biol Phys*. 2007;68(3):771–8.
38. Mansoor A, Bagci U, Foster B, Xu Z, Papadakis GZ, Folio LR, et al. Segmentation and image analysis of abnormal lungs at CT: current approaches, challenges, and future trends. *Radiographics*. 2015;35(4):1056–76.
39. Lee JA. Segmentation of positron emission tomography images: some recommendations for target delineation in radiation oncology. *Radiother Oncol*. 2010;96(3):302–7.
40. Schinagl DA, Span PN, van den Hoogen FJ, Merckx MA, Slootweg PJ, Oyen WJ, et al. Pathology-based validation of FDG PET segmentation tools for volume assessment of lymph node metastases from head and neck cancer. *Eur J Nucl Med Mol Imaging*. 2013;40(12):1828–35.
41. Zaidi H, El Naqa I. PET-guided delineation of radiation therapy treatment volumes: a survey of image segmentation techniques. *Eur J Nucl Med Mol Imaging*. 2010;37(11):2165–87.
42. Drever L, Roa W, McEwan A, Robinson D. Comparison of three image segmentation techniques for target volume delineation in positron emission tomography. *J Appl Clin Med Phys*. 2006;8(Spring 2007):93–109.
43. Abdoli M, Dierckx RA, Zaidi H. Contourlet-based active contour model for PET image segmentation. *Med Phys*. 2013;40(8):082507.
44. Zhuang M, Dierckx RAJO, Zaidi H, eds. Novel active contour model-based automated segmentation of PET images. 2016 IEEE Nuclear Science Symposium, Medical Imaging Conference and Room-Temperature Semiconductor Detector Workshop (NSS/MIC/RTSD); 2016 29 Oct.-6 Nov. 2016.

45. Geets X, Lee JA, Bol A, Lonnew M, Gregoire V. A gradient-based method for segmenting FDG-PET images: methodology and validation. *Eur J Nucl Med Mol Imaging*. 2007;34(9):1427–38.
46. Fonti R, Conson M, Del Vecchio S. PET/CT in radiation oncology. *Semin Oncol*. 2019;46(3):202–9.
47. Belhassen S, Zaidi H. A novel fuzzy C-means algorithm for unsupervised heterogeneous tumor quantification in PET. *Med Phys*. 2010;37(3):1309–24.
48. Konert T, van de Kamer JB, Sonke JJ, Vogel WV. The developing role of FDG PET imaging for prognostication and radiotherapy target volume delineation in non-small cell lung cancer. *J Thorac Dis*. 2018;10(Suppl 21):S2508–S21.
49. Hatt M, Tixier F, Pierce L, Kinahan PE, Le Rest CC, Visvikis D. Characterization of PET/CT images using texture analysis: the past, the present... Any future? *Eur J Nucl Med Mol Imaging*. 2017;44(1):151–65.
50. Yu H, Caldwell C, Mah K, Mozeg D. Coregistered FDG PET/CT-based textural characterization of head and neck cancer for radiation treatment planning. *IEEE Trans Med Imaging*. 2009;28(3):374–83.
51. Huang B, Chen Z, Wu PM, Ye Y, Feng ST, Wong CO, et al. Fully automated delineation of gross tumor volume for head and neck cancer on PET-CT using deep learning: a dual-center study. *Contrast Media Mol Imaging*. 2018;2018:8923028.
52. Guo Z, Guo N, Gong K, Zhong S, Li Q. Gross tumor volume segmentation for head and neck cancer radiotherapy using deep dense multi-modality network. *Phys Med Biol*. 2019;64(20):205015.
53. Hatt M, Lamare F, Bousson N, Turzo A, Collet C, Salzenstein F, et al. Fuzzy hidden Markov chains segmentation for volume determination and quantitation in PET. *Phys Med Biol*. 2007;52(12):3467–91.
54. Hatt M, Lee JA, Schmidtlein CR, Naqa IE, Caldwell C, De Bernardi E, et al. Classification and evaluation strategies of auto-segmentation approaches for PET: report of AAPM task group no. 211. *Med Phys*. 2017;44(6):e1–e42.
55. Hatt M, Cheze le Rest C, Descourt P, Dekker A, De Ruyscher D, Oellers M, et al. Accurate automatic delineation of heterogeneous functional volumes in positron emission tomography for oncology applications. *Int J Radiat Oncol Biol Phys*. 2010;77(1):301–8.
56. Shepherd T, Teras M, Beichel RR, Boellaard R, Bruynooghe M, Dicken V, et al. Comparative study with new accuracy metrics for target volume contouring in PET image guided radiation therapy. *IEEE Trans Med Imaging*. 2012;31(11):2006–24.
57. Rasch C, Belderbos J, van Giersbergen A, De Kok I, Laura T, Boer M, et al. The influence of a multi-disciplinary meeting for quality assurance on target delineation in radiotherapy treatment preparation. *Int J Radiat Oncol*. 2009;75(3):S452–S3.
58. Warfield SK, Zou KH, Wells WM. Simultaneous truth and performance level estimation (STAPLE): an algorithm for the validation of image segmentation. *IEEE Trans Med Imaging*. 2004;23(7):903–21.
59. McGurk RJ, Bowsler J, Lee JA, Das SK. Combining multiple FDG-PET radiotherapy target segmentation methods to reduce the effect of variable performance of individual segmentation methods. *Med Phys*. 2013;40(4):042501.
60. Schaefer A, Vermandel M, Baillet C, Dewalle-Vignion AS, Modzelewski R, Vera P, et al. Impact of consensus contours from multiple PET segmentation methods on the accuracy of functional volume delineation. *Eur J Nucl Med Mol Imaging*. 2016;43(5):911–24.
61. Dewalle-Vignion AS, Betrouni N, Baillet C, Vermandel M. Is STAPLE algorithm confident to assess segmentation methods in PET imaging? *Phys Med Biol*. 2015;60(24):9473–91.
62. Berthon B, Marshall C, Evans M, Spezi E. ATLAAS: an automatic decision tree-based learning algorithm for advanced image segmentation in positron emission tomography. *Phys Med Biol*. 2016;61(13):4855–69.
63. Parkinson C, Evans M, Guerrero-Urbano T, Michaelidou A, Pike L, Barrington S, et al. Machine-learned target volume delineation of (18)F-FDG PET images after one cycle of induction chemotherapy. *Phys Med*. 2019;61:85–93.

64. Das SK, McGurk R, Miften M, Mutic S, Bowsheer J, Bayouth J, et al. Task group 174 report: utilization of [(18) F]fluorodeoxyglucose positron emission tomography ([18) F]FDG-PET) in radiation therapy. *Med Phys*. 2019;46(10):e706–e25.
65. Hallqvist A, Alverbratt C, Strandell A, Samuelsson O, Bjorkander E, Liljegren A, et al. Positron emission tomography and computed tomographic imaging (PET/CT) for dose planning purposes of thoracic radiation with curative intent in lung cancer patients: a systematic review and meta-analysis. *Radiother Oncol*. 2017;123(1):71–7.
66. De Ruyscher D, Wanders S, van Haren E, Hochstenbag M, Geeraedts W, Utama I, et al. Selective mediastinal node irradiation based on FDG-PET scan data in patients with non-small-cell lung cancer: a prospective clinical study. *Int J Radiat Oncol Biol Phys*. 2005;62(4):988–94.
67. Martinussen HM, Reymen B, Wanders R, Troost EG, Dingemans AC, Ollers M, et al. Is selective nodal irradiation in non-small cell lung cancer still safe when using IMRT? Results of a prospective cohort study. *Radiother Oncol*. 2016;121(2):322–7.
68. van Loon J, De Ruyscher D, Wanders R, Boersma L, Simons J, Oellers M, et al. Selective nodal irradiation on basis of (18)FDG-PET scans in limited-disease small-cell lung cancer: a prospective study. *Int J Radiat Oncol Biol Phys*. 2010;77(2):329–36.
69. Faivre-Finn C, Snee M, Ashcroft L, Appel W, Barlesi F, Bhatnagar A, et al. Concurrent once-daily versus twice-daily chemoradiotherapy in patients with limited-stage small-cell lung cancer (CONVERT): an open-label, phase 3, randomised, superiority trial. *Lancet Oncol*. 2017;18(8):1116–25.
70. Nestle U, Schimek-Jasch T, Kremp S, Schaefer-Schuler A, Mix M, Küsters A, et al. Imaging-based target volume reduction in chemoradiotherapy for locally advanced non-small-cell lung cancer (PET-plan): a multicentre, open-label, randomised, controlled trial. *Lancet Oncol*. 2020;21(4):581–92.
71. Nestle U, De Ruyscher D, Ricardi U, Geets X, Belderbos J, Pottgen C, et al. ESTRO ACROP guidelines for target volume definition in the treatment of locally advanced non-small cell lung cancer. *Radiother Oncol*. 2018;127(1):1–5.
72. Vaz SC, Adam JA, Delgado Bolton RC, et al. Joint EANM/SNMMI/ESTRO practice recommendations for the use of 2-[18F]FDG PET/CT external beam radiation treatment planning in lung cancer V1.0. *Eur J Nucl Med Mol Imaging*. 2022;49:1386–406. <https://doi.org/10.1007/s00259-021-05624-5>.
73. Gregoire V, Thorwarth D, Lee JA. Molecular imaging-guided radiotherapy for the treatment of head-and-neck squamous cell carcinoma: does it fulfill the promises? *Semin Radiat Oncol*. 2018;28(1):35–45.
74. Alongi P, Laudicella R, Desideri I, Chiaravalloti A, Borghetti P, Quartuccio N, et al. Positron emission tomography with computed tomography imaging (PET/CT) for the radiotherapy planning definition of the biological target volume: PART 1. *Crit Rev Oncol Hematol*. 2019;140:74–9.
75. Delouya G, Igidbashian L, Houle A, Belair M, Boucher L, Cohade C, et al. (1)(8)F-FDG-PET imaging in radiotherapy tumor volume delineation in treatment of head and neck cancer. *Radiother Oncol*. 2011;101(3):362–8.
76. Paulino AC, Koshy M, Howell R, Schuster D, Davis LW. Comparison of CT- and FDG-PET-defined gross tumor volume in intensity-modulated radiotherapy for head-and-neck cancer. *Int J Radiat Oncol Biol Phys*. 2005;61(5):1385–92.
77. Verma V, Choi JI, Sawant A, Gullapalli RP, Chen W, Alavi A, et al. Use of PET and other functional imaging to guide target delineation in radiation oncology. *Semin Radiat Oncol*. 2018;28(3):171–7.
78. Ciernik IF, Dizendorf E, Baumert BG, Reiner B, Burger C, Davis JB, et al. Radiation treatment planning with an integrated positron emission and computer tomography (PET/CT): a feasibility study. *Int J Radiat Oncol Biol Phys*. 2003;57(3):853–63.
79. Ligtenberg H, Willems SM, Ruiter LN, Jager EA, Terhaard CHJ, Raaijmakers CPJ, et al. Verification of HE-based CTV in laryngeal and hypopharyngeal cancer using pan-cytokeratin. *Clin Transl Radiat Oncol*. 2018;12:21–7.

80. Daisne JF, Duprez T, Weynand B, Lonneux M, Hamoir M, Reyckler H, et al. Tumor volume in pharyngolaryngeal squamous cell carcinoma: comparison at CT, MR imaging, and FDG PET and validation with surgical specimen. *Radiology*. 2004;233(1):93–100.
81. Chatterjee S, Frew J, Mott J, McCallum H, Stevenson P, Maxwell R, et al. Variation in radiotherapy target volume definition, dose to organs at risk and clinical target volumes using anatomic (computed tomography) versus combined anatomic and molecular imaging (positron emission tomography/computed tomography): intensity-modulated radiotherapy delivered using a tomotherapy hi art machine: final results of the VortigERN study. *Clin Oncol (R Coll Radiol)*. 2012;24(10):e173–9.
82. Kyzas PA, Evangelou E, Denaxa-Kyza D, Ioannidis JP. 18F-fluorodeoxyglucose positron emission tomography to evaluate cervical node metastases in patients with head and neck squamous cell carcinoma: a meta-analysis. *J Natl Cancer Inst*. 2008;100(10):712–20.
83. Kim SJ, Pak K, Kim K. Diagnostic accuracy of F-18 FDG PET or PET/CT for detection of lymph node metastasis in clinically node negative head and neck cancer patients; a systematic review and meta-analysis. *Am J Otolaryngol*. 2019;40(2):297–305.
84. Schinagl DA, Hoffmann AL, Vogel WV, van Dalen JA, Verstappen SM, Oyen WJ, et al. Can FDG-PET assist in radiotherapy target volume definition of metastatic lymph nodes in head-and-neck cancer? *Radiother Oncol*. 2009;91(1):95–100.
85. van den Bosch S, Dijkema T, Kunze-Busch MC, Terhaard CH, Raaijmakers CP, Doornaert PA, et al. Uniform FDG-PET guided GRAdient dose prEscription to reduce late radiation toxicity (UPGRADE-RT): study protocol for a randomized clinical trial with dose reduction to the elective neck in head and neck squamous cell carcinoma. *BMC Cancer*. 2017;17(1):208.
86. van den Bosch S, Vogel WV, Raaijmakers CP, Dijkema T, Terhaard CHJ, Al-Mamgani A, et al. Implications of improved diagnostic imaging of small nodal metastases in head and neck cancer: radiotherapy target volume transformation and dose de-escalation. *Radiother Oncol*. 2018;128(3):472–8.
87. Pedraza S, Ruiz-Alonso A, Hernandez-Martinez AC, Cabello E, Lora D, Perez-Regadera JF. (18)F-FDG PET/CT in staging and delineation of radiotherapy volume for head and neck cancer. *Rev Esp Med Nucl Imagen Mol*. 2019;38(3):154–9.
88. Ng SP, Tan J, Osbourne G, Williams L, Bressel MAB, Hicks RJ, et al. Follow up results of a prospective study to evaluate the impact of FDG-PET on CT-based radiotherapy treatment planning for oesophageal cancer. *Clin Transl Radiat Oncol*. 2017;2:76–82.
89. Apolle R, Brückner S, Frosch S, Rehm M, Thiele J, Valentini C, et al. Utility of fiducial markers for target positioning in proton radiotherapy of oesophageal carcinoma. *Radiother Oncol*. 2019;133:28–34.
90. Jimenez-Jimenez E, Mateos P, Aymar N, Roncero R, Ortiz I, Gimenez M, et al. Radiotherapy volume delineation using 18F-FDG-PET/CT modifies gross node volume in patients with oesophageal cancer. *Clin Transl Oncol*. 2018;20(11):1460–6.
91. Cooper JS, Guo MD, Herskovic A, Macdonald JS, Martenson J, James A, Al-Sarraf M, et al. Chemoradiotherapy of locally advanced esophageal Cancer Long-term follow-up of a prospective randomized trial (RTOG 85-01). *JAMA*. 1999;281(17):1623–7.
92. Muijs CT, Beukema JC, Pruijm J, Mul VE, Groen H, Plukker JT, et al. A systematic review on the role of FDG-PET/CT in tumour delineation and radiotherapy planning in patients with esophageal cancer. *Radiother Oncol*. 2010;97(2):165–71.
93. Muijs CT, Beukema JC, Woutersen D, Mul VE, Baveling MJ, Pruijm J, et al. Clinical validation of FDG-PET/CT in the radiation treatment planning for patients with oesophageal cancer. *Radiother Oncol*. 2014;113(2):188–92.
94. Dimopoulos JC, Petrow P, Tanderup K, Petric P, Berger D, Kirisits C, et al. Recommendations from Gynaecological (GYN) GEC-ESTRO working group (IV): basic principles and parameters for MR imaging within the frame of image based adaptive cervix cancer brachytherapy. *Radiother Oncol*. 2012;103(1):113–22.

95. Petrič P, Hudej R, Rogelj P, Blas M, Tanderup K, Fidarova E, et al. Uncertainties of target volume delineation in MRI guided adaptive brachytherapy of cervix cancer: a multi-institutional study. *Radiother Oncol*. 2013;107(1):6–12.
96. Fiorentino A, Laudicella R, Ciurlia E, Annunziata S, Lancellotta V, Mapelli P, et al. Positron emission tomography with computed tomography imaging (PET/CT) for the radiotherapy planning definition of the biological target volume: PART 2. *Crit Rev Oncol Hematol*. 2019;139:117–24.
97. Gandy N, Arshad MA, Park WE, Rockall AG, Barwick TD. FDG-PET imaging in cervical cancer. *Semin Nucl Med*. 2019;49(6):461–70.
98. Adam JA, Arkies H, Hinnen K, Stalpers LJ, van Waesberghe JH, Stoker J, et al. 18F-FDG-PET/CT guided external beam radiotherapy volumes in inoperable uterine cervical cancer. *Q J Nucl Med Mol Imaging*. 2018;62(4):420–8.
99. Adam JA, Loft A, Chagari C, Delgado Bolton RC, Kidd E, Schoder H, et al. EANM/SNMMI practice guideline for [(18)F]FDG PET/CT external beam radiotherapy treatment planning in uterine cervical cancer v1.0. *Eur J Nucl Med Mol Imaging*. 2020;
100. Illidge T, Specht L, Yahalom J, Aleman B, Berthelsen AK, Constine L, et al. Modern radiation therapy for nodal non-Hodgkin lymphoma-target definition and dose guidelines from the international lymphoma radiation oncology group. *Int J Radiat Oncol Biol Phys*. 2014;89(1):49–58.
101. Specht L, Yahalom J, Illidge T, Berthelsen AK, Constine LS, Eich HT, et al. Modern radiation therapy for Hodgkin lymphoma: field and dose guidelines from the international lymphoma radiation oncology group (ILROG). *Int J Radiat Oncol Biol Phys*. 2014;89(4):854–62.
102. Yahalom J, Illidge T, Specht L, Hoppe RT, Li YX, Tsang R, et al. Modern radiation therapy for extranodal lymphomas: field and dose guidelines from the international lymphoma radiation oncology group. *Int J Radiat Oncol Biol Phys*. 2015;92(1):11–31.
103. Specht L, Berthelsen AK. PET/CT in radiation therapy planning. *Semin Nucl Med*. 2018;48(1):67–75.
104. Menon H, Guo C, Verma V, Simone CB 2nd. The role of positron emission tomography imaging in radiotherapy target delineation. *PET Clin*. 2020;15(1):45–53.
105. Sun R, Tang X, Yang Y, Zhang C. (18)FDG-PET/CT for the detection of regional nodal metastasis in patients with head and neck cancer: a meta-analysis. *Oral Oncol*. 2015;51(4):314–20.
106. Hu J, Zhang K, Yan Y, Zang Y, Wang Y, Xue F. Diagnostic accuracy of preoperative (18) F-FDG PET or PET/CT in detecting pelvic and para-aortic lymph node metastasis in patients with endometrial cancer: a systematic review and meta-analysis. *Arch Gynecol Obstet*. 2019;300(3):519–29.
107. Jiang C, Chen Y, Zhu Y, Xu Y. Systematic review and meta-analysis of the accuracy of 18F-FDG PET/CT for detection of regional lymph node metastasis in esophageal squamous cell carcinoma. *J Thorac Dis*. 2018;10(11):6066–76.
108. Li ZZ, Huang YL, Song HJ, Wang YJ, Huang Y. The value of 18F-FDG-PET/CT in the diagnosis of solitary pulmonary nodules: a meta-analysis. *Medicine (Baltimore)*. 2018;97(12):e0130.
109. Schmidt-Hansen M, Baldwin DR, Hasler E, Zamora J, Abairra V, Roque IFM, PET-CT for assessing mediastinal lymph node involvement in patients with suspected resectable non-small cell lung cancer. *Cochrane Database Syst Rev*, 2014(11): p. CD009519. <https://doi.org/10.1002/14651858>. CD009519.pub2.
110. Yu W, Kou C, Bai W, Yu X, Duan R, Zhu B, et al. The diagnostic performance of PET/CT scans for the detection of para-aortic metastatic lymph nodes in patients with cervical cancer: a meta-analysis. *PLoS One*. 2019;14(7):e0220080.
111. Soret M, Bacharach SL, Buvat I. Partial-volume effect in PET tumor imaging. *J Nucl Med*. 2007;48(6):932–45.
112. Surti S. Update on time-of-flight PET imaging. *J Nucl Med*. 2015;56(1):98–105.

113. van der Vos CS, Koopman D, Rijnsdorp S, Arends AJ, Boellaard R, van Dalen JA, et al. Quantification, improvement, and harmonization of small lesion detection with state-of-the-art PET. *Eur J Nucl Med Mol Imaging*. 2017;44(Suppl 1):4–16.
114. van Elmpt W, De Ruyscher D, van der Salm A, Lakeman A, van der Stoep J, Emans D, et al. The PET-boost randomised phase II dose-escalation trial in non-small cell lung cancer. *Radiother Oncol*. 2012;104(1):67–71.
115. van Diessen J, De Ruyscher D, Sonke JJ, Damen E, Sikorska K, Reymen B, et al. The acute and late toxicity results of a randomized phase II dose-escalation trial in non-small cell lung cancer (PET-boost trial). *Radiother Oncol*. 2019;131:166–73.
116. Cooke SA. Local, regional and pulmonary failures in the randomised PET-boost trial for NSCLC patients. 2020 World Conference on Lung Cancer: International Association for the Study of Lung Cancer; 2021.
117. Thorwarth D. Biologically adapted radiation therapy. *Z Med Phys*. 2018;28(3):177–83.
118. van Dijk LV, Noordzij W, Brouwer CL, Boellaard R, Burgerhof JGM, Langendijk JA, et al. (18)F-FDG PET image biomarkers improve prediction of late radiation-induced xerostomia. *Radiother Oncol*. 2018;126(1):89–95.
119. Anthony GJ, Cunliffe A, Castillo R, Pham N, Guerrero T, Armato SG 3rd, et al. Incorporation of pre-therapy (18) F-FDG uptake data with CT texture features into a radiomics model for radiation pneumonitis diagnosis. *Med Phys*. 2017;44(7):3686–94.
120. Zschaecck S, Lock S, Leger S, Haase R, Bandurska-Luque A, Appold S, et al. FDG uptake in normal tissues assessed by PET during treatment has prognostic value for treatment results in head and neck squamous cell carcinomas undergoing radiochemotherapy. *Radiother Oncol*. 2017;122(3):437–44.
121. Zschaecck S, Hofheinz F, Zophel K, Butof R, Jentsch C, Schmollack J, et al. Increased FDG uptake on late-treatment PET in non-tumour-affected oesophagus is prognostic for pathological complete response and disease recurrence in patients undergoing neoadjuvant radiochemotherapy. *Eur J Nucl Med Mol Imaging*. 2017;44(11):1813–22.